

Proceedings of the Institution of Mechanical Engineers, Part C: Journal of Mechanical Engineering Science

<http://pic.sagepub.com/>

Reduced-order modelling in non-linear dynamics: an approach based on non-linear modes

CEN Mazzilli, G C Monticelli and N A Galan Neto

Proceedings of the Institution of Mechanical Engineers, Part C: Journal of Mechanical Engineering Science published online 5 July 2011

DOI: 10.1177/0954406211410267

The online version of this article can be found at:

<http://pic.sagepub.com/content/early/2011/07/05/0954406211410267>

A more recent version of this article was published on - Sep 30, 2011

Published by:



<http://www.sagepublications.com>

On behalf of:



Institution of Mechanical Engineers

Additional services and information for *Proceedings of the Institution of Mechanical Engineers, Part C: Journal of Mechanical Engineering Science* can be found at:

Email Alerts: <http://pic.sagepub.com/cgi/alerts>

Subscriptions: <http://pic.sagepub.com/subscriptions>

Reprints: <http://www.sagepub.com/journalsReprints.nav>

Permissions: <http://www.sagepub.com/journalsPermissions.nav>

[Version of Record](#) - Sep 30, 2011

>> [OnlineFirst Version of Record](#) - Jul 5, 2011

[What is This?](#)

Reduced-order modelling in non-linear dynamics: an approach based on non-linear modes

C E N Mazzilli*, G C Monticelli, and N A Galan Neto

Escola Politécnica, University of São Paulo, São Paulo, Brazil

The manuscript was received on 23 December 2010 and was accepted after revision for publication on 21 April 2011.

DOI: 10.1177/0954406211410267

Abstract: It is largely accepted that non-linear modes of vibration may be particularly suitable for obtaining ‘reduced-order’ models in non-linear dynamics, for their ability to grasp the essential qualitative system information that a much larger number of linear modes are required to. Previous work by the first author on ‘reduced-order’ modelling in non-linear dynamics did not account for the velocity contents within non-linear modes. For many systems, this simplifying assumption does not, in fact, spoil the quality of the ‘reduced-order’ model. Nevertheless, it is not to be generally taken for granted. In this article, a generalised procedure for ‘reduced-order’ modelling in non-linear dynamics that uses the full displacement and velocity contents of non-linear modes is addressed and illustrated. Two case studies are presented and conclusions regarding the relevance of the velocity contents are drawn. Comparison between non-linear dynamic responses of finite-element and ‘reduced-order’ models under different load conditions is made. For both external and parametric resonances, a remarkable agreement between them was achieved, provided the velocity contents within the non-linear modes are retained. In the second case study, damping is essential to help the system settling down in a post-critical periodic attractor, otherwise wave propagation and reflection will have an enduring effect.

Keywords: non-linear dynamics, non-linear modes, non-linear Galerkin method, reduced-order model, parametric resonance

1 INTRODUCTION

In the past two decades, great effort has been made to develop ‘reduced-order’ modelling methodologies in non-linear dynamics, so that adequate qualitative and quantitative representation of ‘high-order’ models might be achieved [1–7]. This was also an issue of particular interest to Steindl and Troger [8], who published a precious synthesis of different approaches used by the beginning of this century. In this article, the subject is recast, to address an improved version of the first author’s earlier work [9, 10], based on the use of non-linear modes to

project the full kinematics onto a low-dimensional subspace, in a non-linear Galerkin fashion.

It is largely accepted that non-linear modes of vibration may be particularly suitable for obtaining ‘reduced-order’ models in non-linear dynamics, for their ability to grasp, even when just a few of them are taken into account, the essential qualitative system information that a much larger number of linear modes is required to [6, 7]. Previous work by the first author [9, 10] on ‘reduced-order’ modelling in non-linear dynamics did not account for the velocity contents that are present in the non-linear normal and multi-modes. It is acknowledged that a few authors have recently considered the velocity terms within non-linear normal modes to obtain ‘reduced-order’ models. That is the case of Touzé and Amabili [6], for whom the ‘non-linear change of co-ordinates’ that allows for the evaluation of the generalised

*Corresponding author: Escola Politécnica da Universidade de São Paulo, Av. Prof. Almeida Prado, Travessa 2 nº 83, 05508-970, São Paulo, Brazil.
email: cenmazzi@usp.br

displacements and velocities of the ‘high-order’ model in terms of the modal co-ordinates of the ‘reduced-order’ model does take the modal velocities into account, for non-gyroscopic systems with elastic non-linearities. A broader class of systems is here considered, since gyroscopic effects and inertial non-linearities may also be included. Still, the purpose of this study goes beyond the consideration of the velocity contents within the non-linear modes to arrive at the ‘reduced-order’ model itself: it is also meant to assess the impact of such terms onto the response, compared to that of displacement-only-based projections, which are standard in non-linear Galerkin procedures. For many systems, this simplifying assumption does not, in fact, spoil the quality of the ‘reduced-order’ model. Nevertheless, this is not to be generally taken for granted, as it will be shown here.

Hence, the purpose of this article is twofold: to pursue a generalised procedure for ‘reduced-order’ modelling in non-linear dynamics that uses the full displacement and velocity contents of non-linear modes and to discuss two case studies envisaging to draw conclusions about the relevance of the velocity contents within the reduction technique.

Although the proposed procedure is also applicable to continuous systems, only discrete systems are here addressed. It is assumed that generalised co-ordinates p_s , $s = 1, 2, \dots, n$ and velocities \dot{p}_s , $s = 1, 2, \dots, n$ describe the ‘high-order’ model kinematics. The equations of motion of a wide class of non-linear discrete systems can be written in the form

$$M_{rs}(\mathbf{p})\ddot{p}_s + D_{rs}(\mathbf{p}, \dot{\mathbf{p}})\dot{p}_s + K_{rs}(\mathbf{p})p_s = R_r, \quad (1)$$

$$r = 1, 2, \dots, n, \quad \text{sum in } s = 1 \text{ to } n$$

where

$$M_{rs}(\mathbf{p}) = M_{rs}^0 + M_{rsk}^1 p_k + M_{rsk\ell}^2 p_k p_\ell$$

$$D_{rs}(\mathbf{p}, \dot{\mathbf{p}}) = D_{rs}^0 + D_{rsk}^1 \dot{p}_k + D_{rsk\ell}^2 \dot{p}_k p_\ell \quad (2)$$

$$K_{rs}(\mathbf{p}) = K_{rs}^0 + K_{rsk}^1 p_k + K_{rsk\ell}^2 p_k p_\ell$$

M_{rs}^0 , M_{rsk}^1 , $M_{rsk\ell}^2$, D_{rs}^0 , D_{rsk}^1 , $D_{rsk\ell}^2$, and K_{rs}^0 , K_{rsk}^1 , $K_{rsk\ell}^2$ are constants defining the (possibly non-linear) matrices of mass, equivalent damping, and stiffness, respectively. Gyroscopic effects can also be considered in $D_{rs}(\mathbf{p}, \dot{\mathbf{p}})$. R_r is a loading vector component. The non-linear equations of motion of a planar frame, for instance, can be put in the form of (1) and (2), as shown in reference [11].

With respect to the ‘reduced-order’ model, it is assumed that the original generalised co-ordinates (p_r , $r = 1, 2, \dots, n$) and velocities (\dot{p}_r , $r = 1, 2, \dots, n$) can be written, up to cubic non-linearities, as functions of the modal displacements U_u and velocities \dot{U}_u , with $u = 1, 2, \dots, m \ll n$,

according to the so-called ‘modal relationships’, corresponding to the ‘non-linear change of co-ordinates’ referred to in [6]

$$p_r(\mathbf{U}, \dot{\mathbf{U}}) = p_{0r} + a_{1r}^u U_u + a_{2r}^u \dot{U}_u + a_{3r}^{uv} U_u U_v + a_{4r}^{uv} U_u \dot{U}_v$$

$$+ a_{5r}^{uv} \dot{U}_u \dot{U}_v + a_{6r}^{uvw} U_u U_v U_w + a_{7r}^{uvw} U_u U_v \dot{U}_w$$

$$+ a_{8r}^{uvw} U_u \dot{U}_v \dot{U}_w + a_{9r}^{uvw} \dot{U}_u \dot{U}_v \dot{U}_w,$$

$$\dot{p}_r(\mathbf{U}, \dot{\mathbf{U}}) = b_{1r}^u U_u + b_{2r}^u \dot{U}_u + b_{3r}^{uv} U_u U_v + b_{4r}^{uv} U_u \dot{U}_v$$

$$+ b_{5r}^{uv} \dot{U}_u \dot{U}_v + b_{6r}^{uvw} U_u U_v U_w + b_{7r}^{uvw} U_u U_v \dot{U}_w$$

$$+ b_{8r}^{uvw} U_u \dot{U}_v \dot{U}_w + b_{9r}^{uvw} \dot{U}_u \dot{U}_v \dot{U}_w, \quad (3)$$

sum in $u, v, w = 1$ to m ; p_{0r} , $r = 1, 2, \dots, n$, stands for the generalised co-ordinate values of the static configuration.

In previous works [9, 10], following the usual trend in non-linear Galerkin procedures, only the displacement-dependent terms $p_r(\mathbf{U}) = p_{0r} + a_{1r}^u U_u + a_{3r}^{uv} U_u U_v + a_{6r}^{uvw} U_u U_v U_w$ have been taken into account to achieve ‘reduced-order’ models, implicitly assuming that the velocity-dependent terms would play a minor role. As already mentioned, in this article the full expression (3) will be used instead, to perform the model reduction. Note that in (3), both the non-linear normal modes and the internally resonant non-linear multi-modes (for which coefficients a ’s and b ’s may be non-null for $u \neq v \neq w$), are included. The next section refers in more detail to the invariant manifold procedure to obtain coefficients a ’s and b ’s.

It is observed that (3) allows for the consideration of any number of non-linear normal modes and/or multi-modes, although it should not be missed that it is always meant to be used the least number of modes that can efficiently represent the original system. A thorough discussion on the criteria to choose the non-linear modes to obtain reliable ‘reduced-order’ models is beyond the present scope, but some comments on the effect of adding new modes are made in Section 3. It could be said that (3) supports a ‘non-linear mode-superposition method’. Of course, such a statement should not be taken as a naïve application of the principle of mode superposition of linear systems theory, which is of course not valid in non-linear dynamics. On the contrary, besides defining the ‘reduced-order’ subspace where non-linear response is assumed, it allows for non-linear contributions of both pure and coupled modes. By the way, an analogous assumption is made in reference [6]. It remains, of course, to detail the procedure that renders the solutions to the non-linear equations of motion of the ‘reduced-order’ model.

2 NON-LINEAR MODAL OSCILLATORS AND MODEL REDUCTION

The origins of non-linear normal modes date back to Lyapunov and Poincaré, but they effectively became a central issue in non-linear dynamics after the works by Rosenberg [12–14], Vakakis [15–17], and Shaw and Pierre [18–20]. Non-linear normal mode, as proposed in references [18–20], is assumed to be a motion restricted to a two-dimensional invariant manifold in the phase space that is tangent to the corresponding eigenplane at the equilibrium state. In a non-linear system, several static equilibrium configurations may co-exist, so that the non-linear normal modes are different for each one of them and are locally valid. In a case of competing equilibrium configurations, the initial conditions become an important issue, since they define in which attracting basin the system will respond and, therefore, which non-linear normal modes should be used in the vicinity of the corresponding equilibrium configuration.

There are different approaches to obtain non-linear normal modes, such as those based on the evaluation of the so-called normal forms [21–23] and those based on the evaluation of the invariant manifolds [18–20] themselves; with regard to the procedures used to determine them, there are those based on analytical methods [24, 25] and a number of different numerical techniques [26, 27]. An extension of the invariant manifold procedure to harmonically driven systems has been recently proposed [28] to take into account its time dependence, which may be required in case of strong non-linearities. Nevertheless, the standard time-independent invariant manifold procedure is here used, since only moderate non-linearities are supposed to occur. In fact, from physical reasoning, Hooke’s law realistically holds for elastic materials while strains are small and displacements are kept within certain bounds. Also, the kinematical approximations implicit in the non-linear beam theory used here are such that both ‘high-order’ and ‘reduced-order’ mathematical models become meaningless outside of those bounds. In other words, while performing parametric analyses, scenarios that drag the mathematical model well beyond those bounds should not be even considered. By the way, the standard time-independent invariant manifolds for harmonically driven systems are also used for ‘reduced-order’ modelling in reference [6].

The set of non-linear second-order differential equations of motion (1) for a ‘high-order’ model has to be converted into a first-order one, using a simple variable transformation, before the invariant manifold that characterises the non-linear normal mode

can be evaluated. This is a costly operation for large ‘high-order’ models, from the computational viewpoint. The ‘modal relationships’ (3) are then introduced into the first-order equations of motion, posing the problem of evaluation of coefficients a ’s and b ’s by solving a set of linear algebraic systems [26]. It is implicit the local validity of the computed non-linear normal modes due to a truncation of (3) in the cubic non-linearities, so that they can be considered accurate only in the vicinity of the equilibrium state, and therefore they are not applicable to strong non-linearities. In cases of internal resonance, a more appropriate extension to non-linear multi-modes should be used [29], so that coupling terms will appear, distinctively of the case of the ‘pure’ normal modes.

Another output of the invariant manifold technique is the equation of motion of the non-linear modal oscillator, which is conveniently expressed in terms of accelerations in (4), after division by the modal mass M_u of the u th mode. It can be written, up to cubic non-linearities, as

$$\begin{aligned} \ddot{U}_u + c_1^u U_u + c_2^u \dot{U}_u + c_3^{uv} U_u U_v + c_4^{uv} U_u \dot{U}_v + c_5^{uv} \dot{U}_u \dot{U}_v \\ + c_6^{uvw} U_u U_v U_w + c_7^{uvw} U_u U_v \dot{U}_w + c_8^{uvw} U_u \dot{U}_v \dot{U}_w \\ + c_9^{uvw} \dot{U}_u \dot{U}_v \dot{U}_w = P_u \end{aligned} \quad (4)$$

where $c_1^u = \omega_{0u}^2$, $c_2^u = 2\xi_u \omega_{0u}$, with ω_{0u} and ξ_u being, respectively, the linear frequency and the modal damping ratio, for free oscillations ($P_u = 0$). Of course, the modal mass M_u can be evaluated in the standard way, as in the linear theory, from $M_u = \sum_r \sum_s (a_{1r}^u)(a_{1s}^u)M_{rs}^0$. Details of the procedure to evaluate coefficients a ’s, b ’s, and c ’s that characterise a non-linear mode can be found in reference [26].

From (3), the virtual generalised displacements can be obtained in terms of the virtual modal displacements

$$\begin{aligned} \delta p_r(\mathbf{U}, \dot{\mathbf{U}}) = [a_{1r}^u + (a_{3r}^{uv} + a_{3r}^{vu})U_v + a_{4r}^{uv}\dot{U}_v \\ + (a_{6r}^{uvw} + a_{6r}^{vuw} + a_{6r}^{wvu})U_v U_w \\ + (a_{7r}^{uvw} + a_{7r}^{vuw})U_v \dot{U}_w + a_{8r}^{uvw}\dot{U}_v \dot{U}_w] \delta U_u \end{aligned} \quad (5)$$

To allow for the characterization of the modal acceleration P_u , in forced systems, the criterion here proposed for model reduction is that the virtual work in the ‘high-order’ model should be equal to that in the ‘reduced-order’ model. Such equality corresponds to a constraint equation, namely that the virtual work, or the ‘energy’, imparted to the modes excluded from the ‘reduced-order’ model should be *zero*, which, of course, is not an exact statement

$$\delta W = \delta \mathbf{p}^T \mathbf{F}_p = \delta \mathbf{U}^T \mathbf{F}_U \quad (6)$$

where \mathbf{F}_p and \mathbf{F}_U stand for the generalised-load vectors, as well as $\delta \mathbf{p}$ and $\delta \mathbf{U}$ stand for the generalised-co-ordinate vectors of the ‘high-order’ and the ‘reduced-order’ model, respectively. With regard to the generalised load R_r , on the right-hand side of (4), the corresponding virtual work term is $R_r \delta p_r = P_u M_u \delta U_u$. Hence, the corresponding modal generalised acceleration P_u can be readily recognised once (5) is used

$$P_u = \gamma_u^r [a_{1r}^u + (a_{3r}^{uv} + a_{3r}^{vu})U_v + a_{4r}^{uw} \dot{U}_v + (a_{6r}^{uvw} + a_{6r}^{vuw} + a_{6r}^{wvu})U_v U_w + (a_{7r}^{uvw} + a_{7r}^{vuw})U_v \dot{U}_w + a_{8r}^{uvw} \dot{U}_v \dot{U}_w] \quad (7)$$

sum in $u, v, w = 1$ to m and $r = 1$ to n . In (7), the following notation was introduced: $\gamma_u^r = R_r/M_u$.

Now, the ‘forced’ modal equations of motion (4), with P_u given by (7), can be integrated and the generalised co-ordinates and velocities of the original model can be recovered from (3). In the case studies that follow, this integration is carried out numerically, using Runge–Kutta’s fourth-order method. Of course, once the ‘reduced-order’ model becomes available, the computational cost of the analyses performed is considerably less than that for the ‘high-order’ model. Nevertheless, the computational cost to evaluate the non-linear modes cannot be underestimated, nor the one to obtain the ‘reduced-order’ model. Direct comparison of computational costs is not, however, the central issue here. Tempting as it may be, ‘reduced-order’ models should not be taken as useful just because they can be qualitatively and quantitatively accurate substitutes for ‘high-order’ models at lower computational cost. They are especially useful because they allow for the application of non-linear dynamics methods to the associated ‘reduced-order’ models, while they are not powerful enough to handle directly the original ‘high-order’ models to perform thorough parametric analyses and identify complex scenarios, in which bifurcations, multiple solutions, erosion of basins of attraction and transition to chaos, among other phenomena may appear. Obviously, once the relevant scenarios have been identified in

the ‘reduced-order’ model, it is highly recommended that the ‘high-order’ model should be recast for the final quantitative analysis.

3 CASE STUDIES

Two case studies are considered, both of them referring to a clamped–free prismatic beam with non-proportional damping, yet with different parameters – cross-section dimensions $b \times h$, damping coefficient c , and loading $R_{14}(t)$, $R_{28}(t)$ or $R_{29}(t)$ –, as depicted in Fig. 1. It is seen from the non-linear modal analysis that internal resonance does not come into play in both the case studies, thus justifying the use of non-linear normal modes.

The ‘high-order’ model with ten beam finite elements of equal length and 30-degrees-of-freedom (p_1 to p_{30}), and the associated ‘reduced-order’ models are discussed. Figure 1 also indicates the generalised co-ordinates p_{29} and p_{30} , respectively, the end-beam transversal displacement and rotation. A two-degree-of-freedom ‘reduced-order’ model is considered in what follows and the modal co-ordinate is chosen to be $U_u = p_{29}$ for both modes $u = 1, 2$.

3.1 First case study

This first case study is concerned with the non-linear response under externally resonant transversal loading. The following parameters are used: $b = 0.010$ m, $h = 0.010$ m, $E = 2.1 \times 10^{11}$ N/m (Young’s modulus), $\rho = 7800$ kg/m³ (specific mass), $c = 0.7$ Ns/m. Here, the loading is comprised by two harmonic forces, which are externally resonant with the second and the first linear modes, respectively: $R_{14}(t) = 6.6 \cos(\omega_{02} t)$ and $R_{29}(t) = 6.6 \cos(\omega_{01} t)$, with values in *Newton* (Fig. 1). The axial load $R_{28}(t)$ is assumed to be null. The first two non-linear normal modes were determined using *MODONL* [26], which is a finite-element code based on the invariant manifold procedure [18–20]. The following non-null

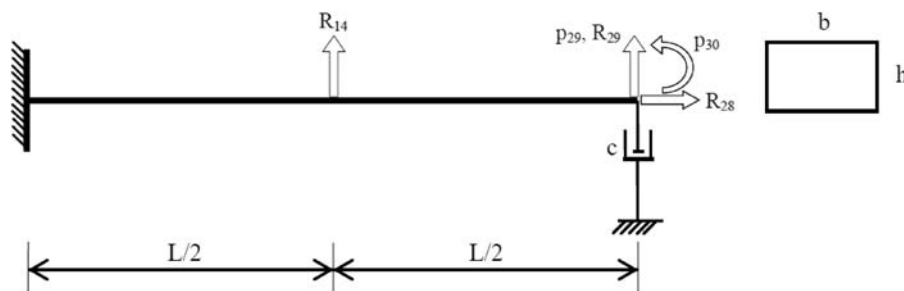


Fig. 1 Clamped–free prismatic beam with dash-pot

coefficients – see (3) and (4) – are obtained for the first mode

$$\begin{aligned} c_1^1 &= 0.17345E + 03 & c_2^1 &= 0.17959E + 01 \\ c_6^{111} &= -0.40506E + 02 & c_7^{111} &= -0.28403E + 00 \\ c_8^{111} &= 0.21383E + 00 & c_9^{111} &= -0.59973E - 03 \\ a_{1,14}^{111} &= 0.33951E + 00 & a_{6,14}^{111} &= -0.57529E - 02 \\ a_{7,14}^{111} &= -0.91501E - 04 & a_{8,14}^{111} &= 0.47231 - 04 \\ a_{1,29}^1 &= 0.10000E + 01 & & \end{aligned}$$

and for the second mode

$$\begin{aligned} c_1^2 &= 0.68055E + 04 & c_2^2 &= 0.17946E + 01 \\ c_6^{222} &= -0.10416E + 06 & c_7^{222} &= 0.18909E + 03 \\ c_8^{222} &= 0.27836E + 02 & c_9^{222} &= -0.93038E - 02 \\ a_{1,14}^{222} &= -0.71314E + 00 & a_{6,14}^{222} &= -0.133399E + 01 \\ a_{7,14}^{222} &= 0.75882E - 02 & a_{8,14}^{222} &= 0.17499E - 03 \\ a_{1,29}^2 &= 0.1000E + 01 & & \end{aligned}$$

The linear natural frequency and the damping ratio for the first mode are $\omega_{01} = \sqrt{c_1^1} = 13.17$ rad/s and $\xi_1 = c_2^1/2\sqrt{c_1^1} = 0.0681$, respectively. For the second mode, the corresponding values are $\omega_{02} = \sqrt{c_1^2} = 82.49$ rad/s and $\xi_2 = c_2^2/2\sqrt{c_1^2} = 0.0108$. By the way, due to the fact that this is not a system with proportional damping, the modes are not, strictly speaking, standing waves. This is particularly seen to be the case of the second mode [26].

It can be readily observed that the modal oscillator equation of the first mode contains important cubic non-linearities – $c_6^{111}(U_1)^3 + c_7^{111}(U_1)^2\dot{U}_1 +$

$c_8^{111}U_1(\dot{U}_1)^2 + c_9^{111}(\dot{U}_1)^3$ – but the modal load P_1 is basically dominated by the linear terms – $\gamma_1^{14}a_{1,14}^1 + \gamma_1^{29}a_{1,29}^1$ – since the non-linearities – $\gamma_1^{14}[3a_{6,14}^{111}(U_1)^2 + 2a_{7,14}^{111}U_1\dot{U}_1 + a_{8,14}^{111}(\dot{U}_1)^2]$ – are relatively weak. As for the second-mode oscillator equation, besides the cubic non-linearities – $c_6^{222}(U_2)^3 + c_7^{222}(U_2)^2\dot{U}_2 + c_8^{222}U_2(\dot{U}_2)^2 + c_9^{222}(\dot{U}_2)^3$, the modal load P_2 , in addition to the linear terms – $\gamma_2^{14}a_{1,14}^2 + \gamma_2^{29}a_{1,29}^2$, is also strongly influenced by non-linear terms – $\gamma_2^{14} \times [3a_{6,14}^{222}(U_2)^2 + 2a_{7,14}^{222}U_2\dot{U}_2 + a_{8,14}^{222}(\dot{U}_2)^2]$. It should be recalled that the order of magnitude of the modal velocity $O(\dot{U}_u)$ is much larger than that of the modal displacement $O(U_u)$, since $O(\dot{U}_u) = \omega_{0u}O(U_u)$, which leads to non-linearly-amplified velocity-dependent terms particularly in the second mode, because $\omega_{02} = 82.49$ rad/s is large. The relevance of velocity-dependent terms in the response of the ‘reduced-order’ model goes beyond this: in fact, if only displacement-dependent terms were considered, a softening behaviour would be anticipated, due to the negative value of both c_6^{111} and c_6^{222} ; nevertheless, the velocity-dependent terms can affect that conclusion, both quantitatively and qualitatively, including a hardening possibility.

For both modes, the modal masses in this particular case study coincidentally happen to be equal ($M_1 = M_2 = 0.44$ kg). Hence, the applied loading can be characterised by same-amplitude accelerations $\gamma_1^{14} = \gamma_2^{14} = \gamma_0 \cos(82.2 t)$ and $\gamma_1^{29} = \gamma_2^{29} = \gamma_0 \cos(13.17 t)$, with $\gamma_0 = 15$ m/s². Figure 2 displays

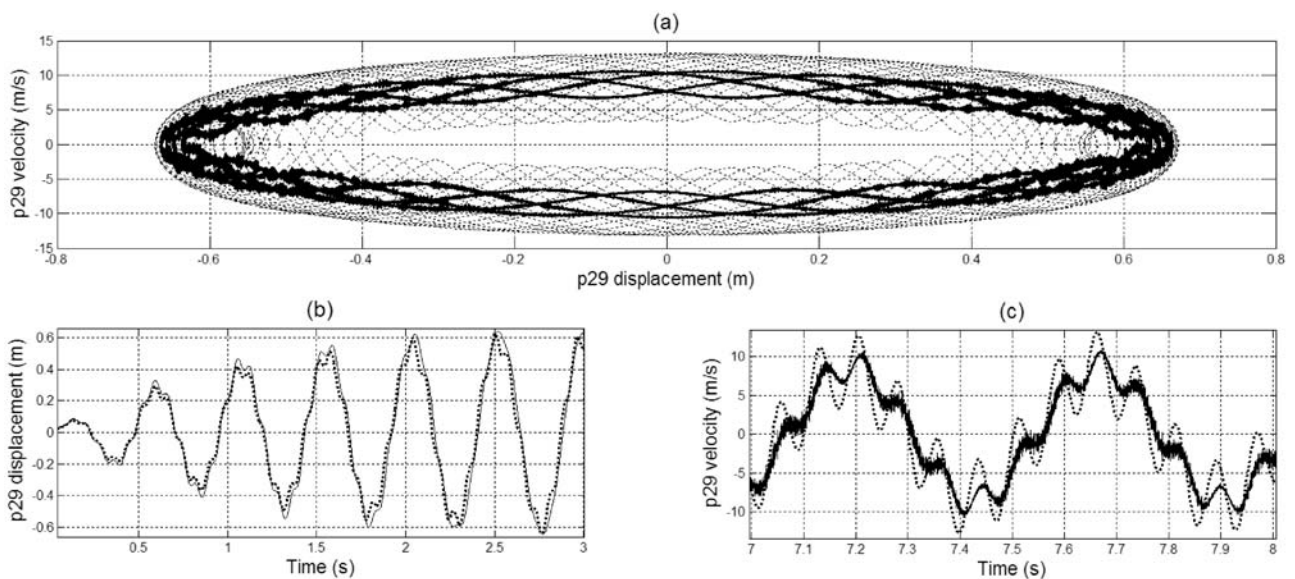


Fig. 2 p_{29} and \dot{p}_{29} modal-variable comparison between the ANDROS (full line) and the total response of the ‘reduced-order’ model (dashed line): (a) the projection onto the phase plane $\dot{p}_{29} \times p_{29}$; (b) p_{29} time response; and (c) \dot{p}_{29} time response, $\gamma_0 = 15$ m/s²

the results obtained for p_{29} and shows that the 'reduced-order' model compares surprisingly well with the finite-element model, even for displacements that are not small, using *ANDROS* [11], which is a non-linear finite-element time-domain analysis code that uses the same beam theory. In fact, deviations of the order of only 1 per cent for the maximum amplitudes are observed. Of course, neither the finite-element solution nor the 'reduced-order' model can be claimed to be 'exact', so that error estimations are not made, just deviations between them are computed. Nevertheless, it should be reckoned that, in spite of a very good agreement for displacements, differences are noticeable in the phase-plane projection $\dot{p}_{29} \times p_{29}$ due to the poorer approximation in the velocity field, which anyhow should be expected both in the 'reduced-order' and in the finite-element approximations. Further, the velocity time-response plot shows that the 'reduced-order' model is obviously able to capture contributions from the only-two modes used, while the finite-element solution reveals a 'dirtier' signal and a much more complex modal combination. Nevertheless, the two models describe a similar transient regime and reach basically the same amplitudes and periods in the quasi-steady state, thus allowing inferring that the 'reduced-order' model is an adequate representation of the 'high-order' model. The steady-state solution is seen to be insensitive to initial conditions.

When the modal relationships (3) are used, any other generalised co-ordinate and velocity of the 'high-order' model can be recovered, provided both the modal displacement and velocity are known. To illustrate it, the p_{30} generalised co-ordinate is considered. From (3)

$$\begin{aligned} p_{30} = & a_{1,30}^1 U_1 + a_{1,30}^2 U_2 + a_{2,30}^1 \dot{U}_1 + a_{2,30}^2 \dot{U}_2 + a_{3,30}^{11} (U_1)^2 \\ & + a_{3,30}^{22} (U_1)^2 + a_{4,30}^{11} U_1 \dot{U}_1 + a_{4,30}^{22} U_2 \dot{U}_2 + a_{5,30}^{11} (\dot{U}_1)^2 \\ & + a_{5,30}^{22} (\dot{U}_2)^2 + a_{6,30}^{111} (U_1)^3 + a_{6,30}^{222} (U_2)^3 + a_{7,30}^{111} (U_1)^2 \dot{U}_1 \\ & + a_{7,30}^{222} (U_2)^2 \dot{U}_2 + a_{8,30}^{111} U_1 (\dot{U}_1)^2 + a_{8,30}^{222} U_2 (\dot{U}_2)^2 \\ & + a_{9,30}^{111} (\dot{U}_1)^3 + a_{9,30}^{222} (\dot{U}_2)^3 \end{aligned}$$

$$\begin{aligned} \dot{p}_{30} = & b_{1,30}^1 U_1 + b_{1,30}^2 U_2 + b_{2,30}^1 \dot{U}_1 + b_{2,30}^2 \dot{U}_2 + b_{3,30}^{11} (U_1)^2 \\ & + b_{3,30}^{22} (U_1)^2 + b_{4,30}^{11} U_1 \dot{U}_1 + b_{4,30}^{22} U_2 \dot{U}_2 + b_{5,30}^{11} (\dot{U}_1)^2 \\ & + b_{5,30}^{22} (\dot{U}_2)^2 + b_{6,30}^{111} (U_1)^3 + b_{6,30}^{222} (U_2)^3 + b_{7,30}^{111} (U_1)^2 \dot{U}_1 \\ & + b_{7,30}^{222} (U_2)^2 \dot{U}_2 + b_{8,30}^{111} U_1 (\dot{U}_1)^2 + b_{8,30}^{222} U_2 (\dot{U}_2)^2 \\ & + b_{9,30}^{111} (\dot{U}_1)^3 + b_{9,30}^{222} (\dot{U}_2)^3 \end{aligned}$$

with the following non-null coefficients, from *MODONL* [26], for the first mode

$$\begin{aligned} a_{1,30}^1 &= 0.68828E + 00 & a_{2,30}^1 &= -0.67052E - 03 \\ a_{6,30}^{111} &= 0.76285E - 02 & a_{7,30}^{111} &= 0.13231E - 03 \\ a_{8,30}^{111} &= -0.69597E - 04 & & \\ b_{1,30}^1 &= 0.11630E + 00 & b_{2,30}^1 &= 0.68948E + 00 \\ b_{6,30}^{111} &= -0.50102E - 01 & b_{7,30}^{111} &= 0.46600E - 01 \\ b_{8,30}^{111} &= 0.69290E - 03 & b_{9,30}^{111} &= -0.69117E - 04 \end{aligned}$$

and for the second mode

$$\begin{aligned} a_{1,30}^2 &= 0.23896E + 01 & a_{2,30}^2 &= -0.59586E - 03 \\ a_{6,30}^{222} &= 0.20454E + 00 & a_{7,30}^{222} &= -0.28702E - 02 \\ a_{8,30}^{222} &= 0.63985E - 03 & & \\ b_{1,30}^2 &= 0.40551E + 01 & b_{2,30}^2 &= 0.23907E + 01 \\ b_{6,30}^{222} &= -0.42533E + 02 & b_{7,30}^{222} &= -0.79776E + 01 \\ b_{8,30}^{222} &= 0.17033E - 01 & b_{9,30}^{222} &= 0.63941E - 03 \end{aligned}$$

It is seen that, besides the linear terms, there is only one non-linearity with (a moderate) influence on the p_{30} response, namely $a_{8,30}^{222} U_2 (\dot{U}_2)^2$, which is a second-mode contribution. Still, for \dot{p}_{30} , besides the linear terms, there are non-linear relevant contributions, $b_{6,30}^{222} (U_2)^3 + b_{7,30}^{222} (U_2)^2 \dot{U}_2 + b_{8,30}^{222} U_2 (\dot{U}_2)^2 + b_{9,30}^{222} (\dot{U}_2)^3$, which are also associated to the second mode. It should be again recalled that $O(\dot{U}_u) = \omega_{0u} O(U_u)$, which leads to non-linearly-amplified velocity-dependent terms particularly in the second mode, because $\omega_{02} = 82.49$ rad/s is large.

Figure 3 displays the results for p_{30} and \dot{p}_{30} , which are evaluated for the 'reduced-order' model as in (3), after the forced modal oscillator equations (4) have been numerically integrated.

It is seen from Fig. 3(c) that the total velocity response $\dot{p}_{30}(t)$ indicates a modulated pattern, as a result of the composition of two non-commensurable harmonic contributions, resulting in a strictly-speaking non-periodic function. Figure 3(c) separately depicts the forced response for the first and the second non-linear modes, together with the total response obtained by the 'non-linear mode superposition', as proposed in (3). As already mentioned, the first mode is dominated by the linear terms, leading to the typical 'elliptical' closed orbits in the phase plane projection $\dot{p}_{30} \times p_{30}$. For the second mode, the relevant cubic non-linearities introduce a 'bouncing' effect about an average 'elliptical' phase trajectory. Comparison with finite-element results, using *ANDROS* [11], reveals a good qualitative agreement, although with deviations of the order of 14 per cent for the maximum p_{30} displacements, which is understandably larger than that obtained for the modal co-ordinate p_{29} . It should be recalled that a propagation error is expected within the modal relationships (3).

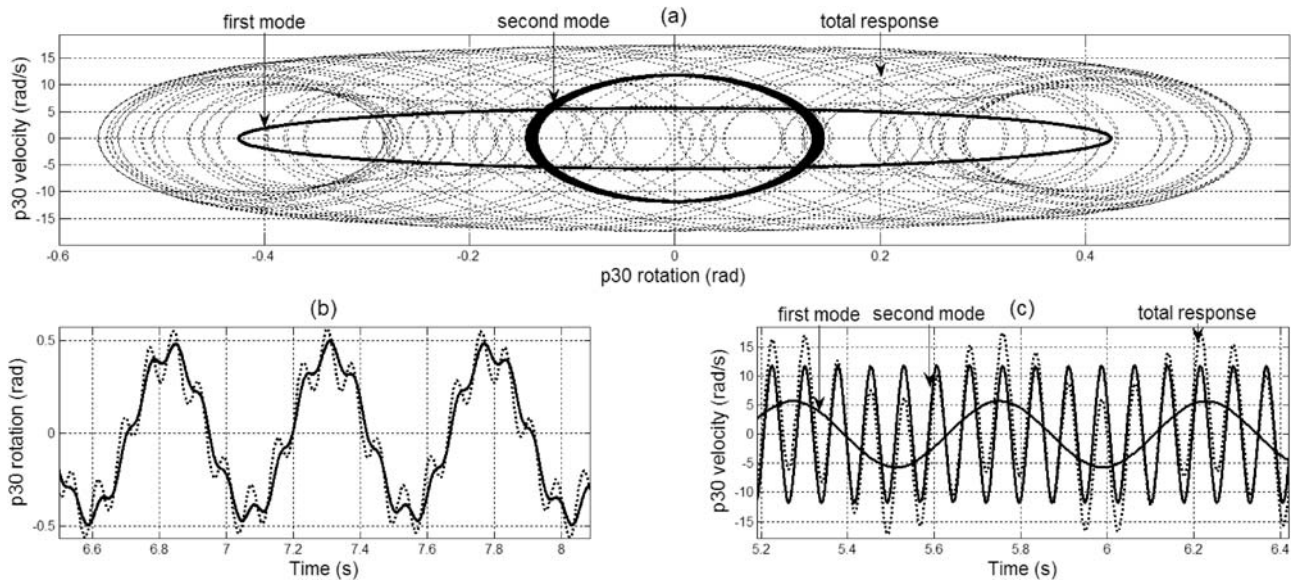


Fig. 3 (a) The projection onto the phase plane $\dot{p}_{30} \times p_{30}$ of the first mode, the second mode and the total response of the ‘reduced-order’ model; (b) p_{30} time response comparison between the ANDROS (full line) and the total response of the ‘reduced-order’ model (dashed line); and (c) \dot{p}_{30} time response of the first mode, the second mode and the total response of the ‘reduced-order’ model, $\gamma_0 = 15 \text{ m/s}^2$

Finally, to assess the role played by the velocity-dependent terms within the non-linear modes, when it comes to obtain ‘reduced-order’ models, a comparison is shown in Fig. 4 between results with and without it.

Non-negligible deviations – as large as 8 per cent – for maximum displacements can be observed in Fig. 4, thus justifying the use of the improved procedure for ‘reduced-order’ modelling. Deviations should, of course, be much smaller if the structure were not so slender, so lightly damped and also subjected to external resonance. Still, the improved procedure to obtain ‘reduced-order’ models is not much more laborious and renders more reliable results than the previously proposed one [9, 10], so that it should be used even when the scenario is not as critical as the one addressed here.

3.2 Second case study

As a second case study (Fig. 1), a much slender clamped-free beam subjected to a harmonic axial load $R_{28}(t) = 1.62 \cos(2\omega_0 t)$, values in *Newton*, is considered with twice the frequency of either the first ($u=1$) or the second mode ($u=2$), so that the system may be driven into parametric resonance [30]. Now, it is assumed that $R_{14}(t) = R_{29}(t) = 0$. The following parameters are used: $b = 0.040 \text{ m}$, $h = 0.003 \text{ m}$, $E = 2.1 \times 10^{11} \text{ N/m}$ (Young’s modulus), $\rho = 7800 \text{ kg/m}^3$ (specific mass). As before, a two-degree-of-freedom ‘reduced-order’ model is

considered and the modal co-ordinate is chosen to be $U_u = p_{29}$ for both modes $u = 1, 2$.

Assuming initially the system to be undamped, $c = 0$, the first non-linear mode is characterised by the following non-null coefficients, which define the modal oscillator equation (4) and the modal relationships (3), according to MODONL [26]

$$\begin{aligned} c_1^1 &= 0.15602E + 02 & c_6^{111} &= 0.53036E + 00 \\ c_8^{111} &= 0.28812E + 00 \\ a_{3,28}^{11} &= -0.29049E + 00. \end{aligned}$$

Analogously, for the second mode, the following non-null coefficients are obtained, according to MODONL [26]

$$\begin{aligned} c_1^2 &= 0.61277E + 03 & c_6^{222} &= -0.93646E + 04 \\ c_8^{222} &= 0.27923E + 02 \\ a_{3,28}^{22} &= -0.20261E + 01 \end{aligned}$$

Now, the linear natural frequencies for the first and second modes are $\omega_{01} = \sqrt{c_1^1} = 3.95 \text{ rad/s}$ and $\omega_{02} = \sqrt{c_1^2} = 24.75 \text{ rad/s}$, respectively.

It is readily seen that the modal-oscillator equation of the first mode contains important cubic non-linearities – $c_6^{111}(U_1)^3 + c_8^{111}U_1(\dot{U}_1)^2$ and the modal load P_1 is strongly dominated by a non-linear term – $\gamma_1^{28}a_{3,28}^{11}U_1$. Analogously, for the second mode, besides the cubic non-linearities in the oscillator equation – $c_6^{222}(U_2)^3 + c_8^{222}U_2(\dot{U}_2)^2$, the modal load P_2 is also strongly influenced by a non-linear term – $\gamma_2^{28}a_{3,28}^{22}U_2$. It should be recalled that

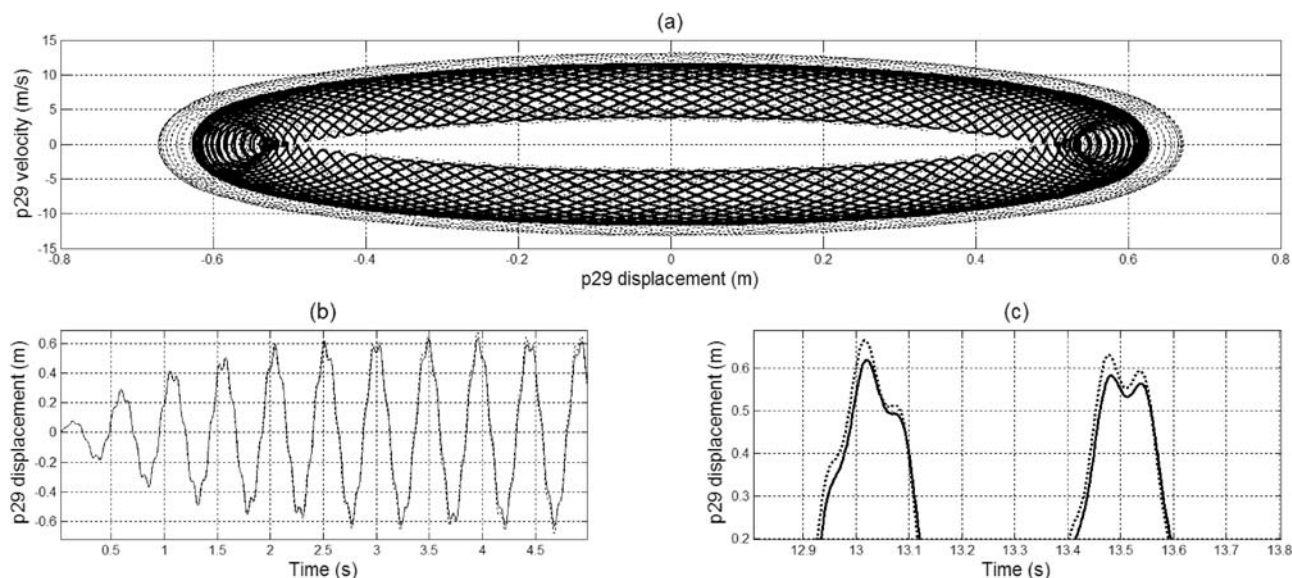


Fig. 4 p_{29} and \dot{p}_{29} modal-variable comparison of the total response considering a ‘reduced-order’ model with (dashed line) or without (full line) velocity contents in the non-linear mode: (a) the projection onto the phase plane $\dot{p}_{29} \times p_{29}$; (b) p_{29} time response; and (c) zooming for time response, $\gamma_0 = 15 \text{ m/s}^2$

$O(\dot{U}_u) = \omega_{0u}O(U_u)$, which leads to non-linearly-amplified velocity-dependent terms particularly in the second mode, because $\omega_{02} = 24.75 \text{ rad/s}$ is large. Again, the relevance of velocity-dependent terms in the response of the ‘reduced-order’ model goes beyond this: in fact, if only displacement-dependent terms were considered, a first mode with hardening and a second mode with softening would be anticipated, due to a positive c_6^{111} and a negative c_6^{222} ; nevertheless, the velocity-dependent terms can affect this conclusion, both quantitatively and qualitatively.

For both modes, the modal masses in this particular case study coincidentally happen to be equal ($M_1 = M_2 = 0.54 \text{ kg}$). Hence, the applied load $R_{28}(t) = 1.62 \cos(2\omega_{0u}t)$ can be characterised by same-amplitude modal accelerations $\gamma_u^{28} = \gamma_0 \cos 2\omega_{0u}t$, $u = 1, 2$, with $\gamma_0 = 3.0 \text{ m/s}^2$. Figure 5 displays the results obtained for p_{29} , when either the first or the second mode is subjected to parametric excitation. It also shows that the results of the ‘reduced-order’ model compare well with those from the finite-element analysis, using *ANDROS* [11], even for relatively large displacements.

With respect to the parametric resonance with the first mode, it is seen from Fig. 5 that both the ‘high-order’ and the ‘reduced-order’ models present similar ‘pulses’, with very close maximum displacements (deviation of 2 per cent). It is noticeable, however, that the finite-element model indicates a ‘jammed’

pattern, which could probably be explained by the composition of incoming and reflected longitudinal waves. Hence, it seems that the ‘reduced-order’ model was not able to fully capture the wave propagation effects for the undamped model. It is also noticeable that the non-linear response of the ‘reduced-order’ model ‘awakes’ sooner than that of the finite-element analysis. Similar conclusions can be drawn for the parametric resonance with respect to the second mode, although a larger relative deviation (34 per cent) is observed for the maximum displacements, which are nevertheless much smaller (and therefore less important) than those for the parametric resonance of the first mode. It also takes much longer for the finite-element response to build up, which probably indicates the influence of numerical damping.

When the ‘modal relationships’ (3) are used, any other generalised co-ordinate and velocity of the ‘high-order’ model can be recovered, provided the modal displacement and velocity are known. To illustrate it, the p_{30} generalised co-ordinate is considered. From (3)

$$\begin{aligned}
 p_{30} = & a_{1,30}^1 U_1 + a_{1,30}^2 U_2 + a_{2,30}^1 \dot{U}_1 + a_{2,30}^2 \dot{U}_2 + a_{3,30}^{11} (U_1)^2 \\
 & + a_{3,30}^{22} (U_2)^2 + a_{4,30}^{11} U_1 \dot{U}_1 + a_{4,30}^{22} U_2 \dot{U}_2 + a_{5,30}^{11} (\dot{U}_1)^2 \\
 & + a_{5,30}^{22} (\dot{U}_2)^2 + a_{6,30}^{111} (U_1)^3 + a_{6,30}^{222} (U_2)^3 + a_{7,30}^{111} (U_1)^2 \dot{U}_1 \\
 & + a_{7,30}^{222} (U_2)^2 \dot{U}_2 + a_{8,30}^{111} U_1 (\dot{U}_1)^2 + a_{8,30}^{222} U_2 (\dot{U}_2)^2 \\
 & + a_{9,30}^{111} (\dot{U}_1)^3 + a_{9,30}^{222} (\dot{U}_2)^3
 \end{aligned}$$

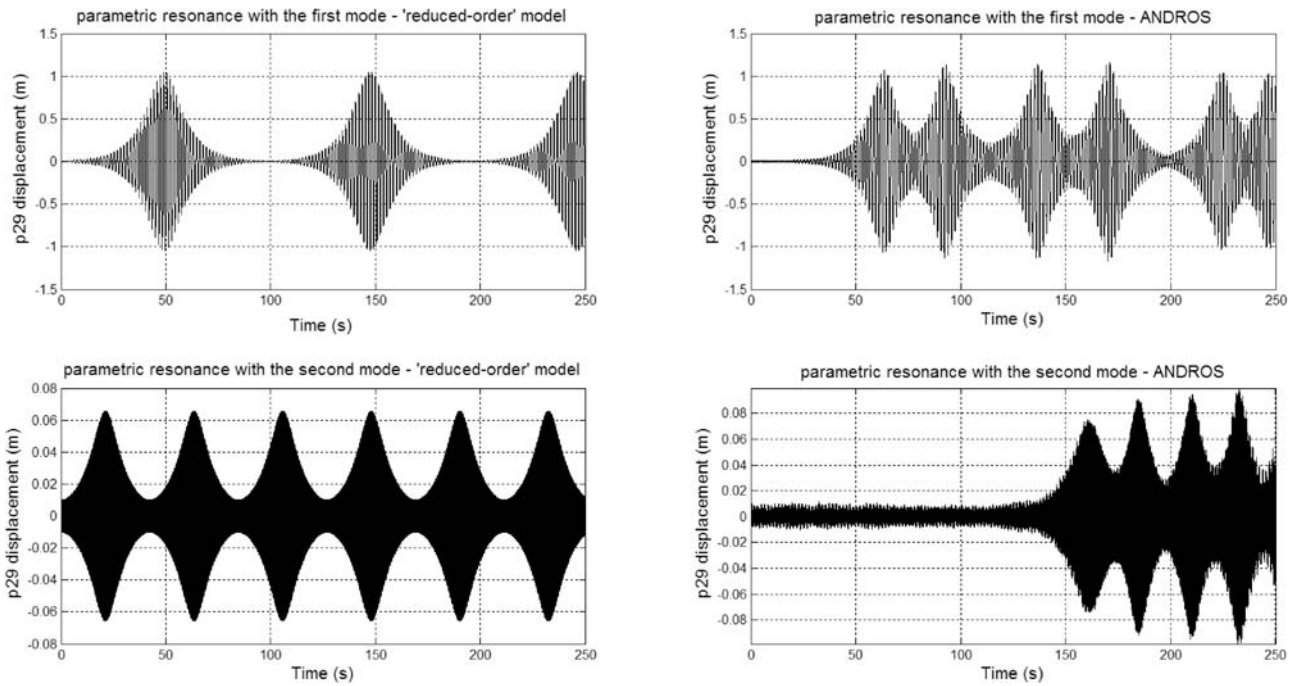


Fig. 5 p_{29} in the ‘reduced-order’ model and *ANDROS*, for parametric resonance with respect to the first or the second mode, $c = 0$ Ns/m, $\gamma_0 = 3.0$ m/s²

$$\begin{aligned} \dot{p}_{30} = & b_{1,30}^1 U_1 + b_{1,30}^2 U_2 + b_{2,30}^1 \dot{U}_1 + b_{2,30}^2 \dot{U}_2 + b_{3,30}^{11} (U_1)^2 \\ & + b_{3,30}^{22} (U_1)^2 + b_{4,30}^{11} U_1 \dot{U}_1 + b_{4,30}^{22} U_2 \dot{U}_2 + b_{5,30}^{11} (\dot{U}_1)^2 \\ & + b_{5,30}^{22} (\dot{U}_2)^2 + b_{6,30}^{111} (U_1)^3 + b_{6,30}^{222} (U_2)^3 + b_{7,30}^{111} (U_1)^2 \dot{U}_1 \\ & + b_{7,30}^{222} (U_2)^2 \dot{U}_2 + b_{8,30}^{111} U_1 (\dot{U}_1)^2 + b_{8,30}^{222} U_2 (\dot{U}_2)^2 \\ & + b_{9,30}^{111} (\dot{U}_1)^3 + b_{9,30}^{222} (\dot{U}_2)^3 \end{aligned}$$

with the following non-null coefficients, from *MODONL* [26], for the first mode

$$\begin{aligned} a_{1,30}^1 &= 0.68825E + 00 & a_{6,30}^{111} &= -0.14670E - 01 \\ a_{8,30}^{111} &= -0.57711E - 03 \\ b_{2,30}^1 &= 0.68825E + 00 & b_{7,30}^{111} &= -0.26003E - 01 \\ b_{9,30}^{111} &= -0.57711E - 03 \end{aligned}$$

and for the second mode

$$\begin{aligned} a_{1,30}^2 &= 0.23904E + 01 & a_{6,30}^{222} &= -0.18395E + 00 \\ a_{8,30}^{222} &= -0.70873E - 02 \\ b_{2,30}^2 &= 0.23904E + 01 & b_{7,30}^{222} &= -0.81339E + 01 \\ b_{9,30}^{222} &= -0.70873E - 02 \end{aligned}$$

For parametric resonance with the first mode, it is seen that the linear term prevails in the p_{30} response. The non-linear terms $-a_{6,30}^{111} (U_1)^3 + a_{8,30}^{111} U_1 (\dot{U}_1)^2$ have just a moderate influence on it. Still, for \dot{p}_{30} , besides the linear term, the non-linearities $-b_{7,30}^{111} (U_1)^2 \dot{U}_1 + b_{9,30}^{111} (\dot{U}_1)^3$ become relevant. For parametric resonance with the second mode, besides the linear term, non-linearities $-a_{6,30}^{222} (U_2)^3 + a_{8,30}^{222} U_2 (\dot{U}_2)^2$ have a pronounced influence on the p_{30} response.

Further, for \dot{p}_{30} , besides the linear term, the non-linearities $-b_{7,30}^{222} (U_2)^2 \dot{U}_2 + b_{9,30}^{222} (\dot{U}_2)^3$ are important. It should be recalled that $O(\dot{U}_u) = \omega_{0u} O(U_u)$, which leads to non-linearly-amplified velocity-dependent terms particularly in the second mode, because $\omega_{02} = 24.75$ rad/s is large.

Figure 6 displays the results for p_{30} and \dot{p}_{30} , which are evaluated for the ‘reduced-order’ model as in (3), after the forced modal oscillator equations (4) have been integrated, and for the finite-element model using *ANDROS* [11].

Again, the ‘reduced-order’ model gives satisfactory results when compared to *ANDROS* [11], the main conclusions being similar to those mentioned for Fig. 5, with respect to the amplitudes and ‘jammed’ patterns. Deviations in the maximum amplitudes were of the order of 11 per cent and 44 per cent, for parametric resonance with respect to the first and the second modes, respectively. As already pointed out, a propagation error is expected when the modal relationships (3) are used to evaluate an original generalised co-ordinate (such as p_{30}) in terms of the modal co-ordinate (p_{29}). That is why the deviations just found are larger than those of Fig. 5.

Finally, to assess the role played by the velocity contents within the non-linear modes, when it comes to obtain ‘reduced-order’ models, a comparison is shown in Fig. 7 between results with and without it.

Deviations as large as 50 per cent for the maximum amplitudes and 17 per cent for the modulation period can be observed in Fig. 7, thus justifying the use of the

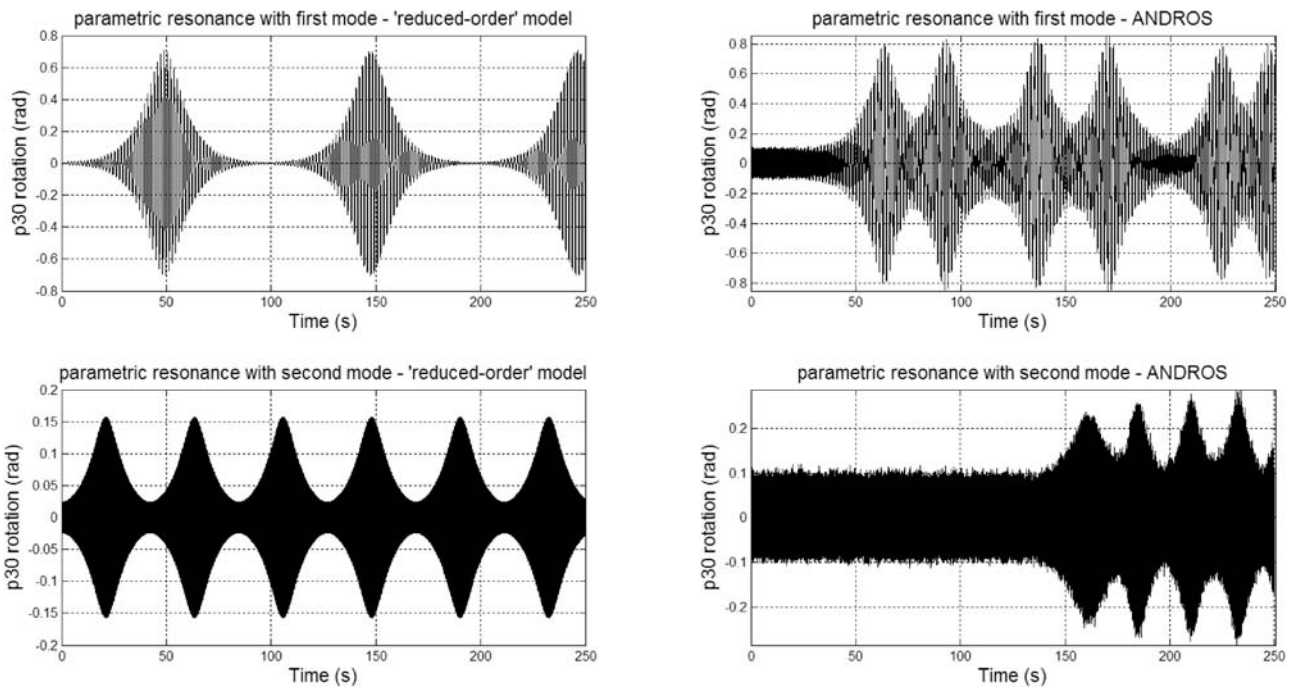


Fig. 6 $p_{30}(t)$ in the ‘reduced-order’ model and *ANDROS*, for parametric resonance with respect to the first or the second mode, $c = 0$, $\gamma_0 = 3.0 \text{ m/s}^2$

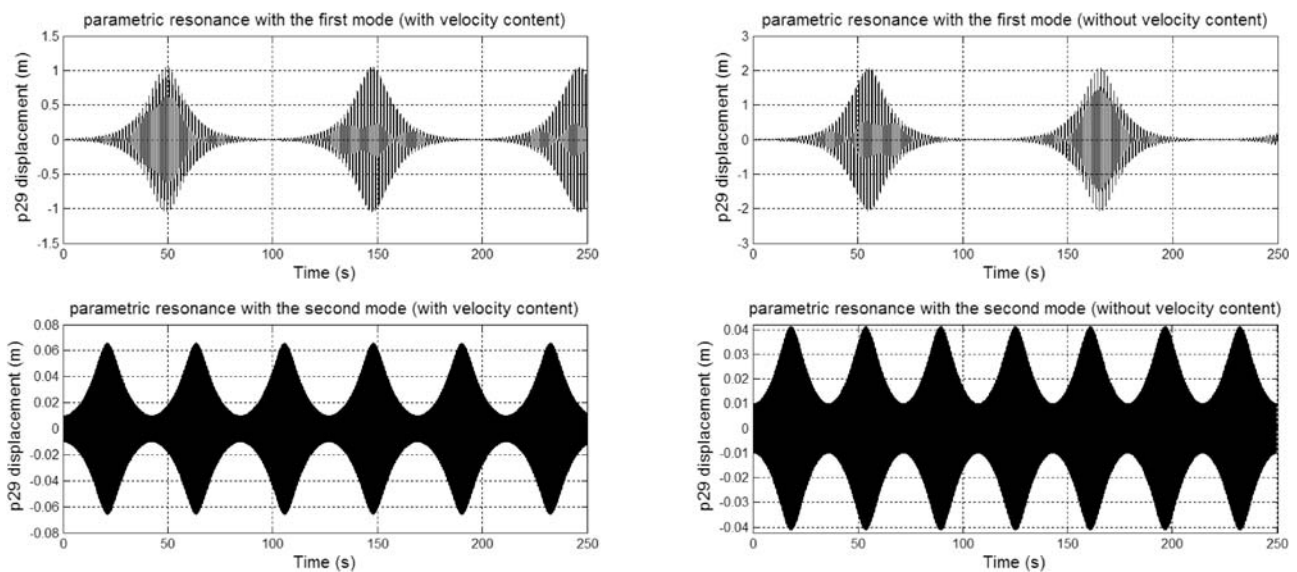


Fig. 7 p_{29} in the ‘reduced-order’ model with or without velocity contents in the non-linear mode, for parametric resonance with respect to the first or the second mode, $c = 0$, $\gamma_0 = 3.0 \text{ m/s}^2$

improved procedure for ‘reduced-order’ modelling. Velocity-dependent terms in the non-linear modes may act either to decrease (for the parametric resonance with respect to the first mode) or increase (for the parametric resonance with respect to the second mode) the response amplitudes. Deviations should, of course, be much smaller if the structure were not so slender, undamped and also subjected to parametric

resonance. Still, the improved procedure to obtain ‘reduced-order’ models is not much more laborious and renders more reliable results than the previously proposed one [9, 10], so that it should be used even when the scenario is not as critical as the one addressed here.

Considering now the case of a lightly damped system, $c = 0.01 \text{ Ns/m}$, the first non-linear mode is

characterised by the following non-null coefficients, which define the modal oscillator equation (4) and the modal relationships (3), according to *MODONL* [26]

$$\begin{aligned} c_1^1 &= 0.15602E + 02 & c_2^1 &= 0.21368E - 01 \\ c_6^{111} &= 0.53032E + 00 & c_7^{111} &= -0.50348E - 02 \\ c_8^{111} &= 0.28812E + 00 \\ a_{3,28}^{11} &= -0.29049E + 00 \end{aligned}$$

Analogously, for the second mode, the following non-null coefficients are obtained, according to *MODONL* [26]

$$\begin{aligned} c_1^2 &= 0.61277E + 03 & c_2^2 &= 0.21370E - 01 \\ c_6^{222} &= -0.93645E + 04 & c_7^{222} &= 0.22620E + 01 \\ c_8^{222} &= 0.27923E + 02 \\ a_{3,28}^{22} &= -0.20261E + 01 \end{aligned}$$

Now, the linear natural frequency and the damping ratio are, respectively, $\omega_{01} = \sqrt{c_1^1} = 3.95$ rad/s and $\xi_1 = c_2^1/2\sqrt{c_1^1} = 0.002$, for the first mode, and $\omega_{02} = \sqrt{c_1^2} = 24.75$ rad/s and $\xi_2 = c_2^2/2\sqrt{c_1^2} = 0.0005$, for the second mode. The same comments of the undamped case with regard to the relevant non-linear terms in the modal-oscillator equation and the modal load apply here.

Figure 8 displays the results obtained for p_{29} , when either the first or the second mode is subjected to parametric excitation. It also shows that the ‘reduced-order’ model results compare qualitatively well with those from the finite-element analysis, using *ANDROS* [11], since both models were able to capture a periodic attractor, and quantitatively reasonably well, even for relatively large displacements (9 per cent and 27 per cent deviations for parametric resonance with respect to the first or the second modes, respectively).

With respect to the parametric resonance with the first mode, it is seen from Fig. 8 that both the ‘high-order’ and the ‘reduced-order’ models present almost the same pulse pattern, while approaching a periodic attractor, with very close maximum displacements. This periodic attractor is in contrast with the undamped case (Fig. 5). Damping, light as it may be, eases the attainment of a periodic attractor and smoothens the incoming and reflected wave pulses. On the other hand, larger damping might kill the non-linear periodic attractor. Therefore, for this lightly damped system the ‘reduced-order’ model was able to adequately capture wave propagation effects. It is again noticeable that the non-linear response of the ‘reduced-order’ model ‘awakes’ sooner than that of the finite-element model. Similar conclusions can be drawn for the parametric resonance with respect to the second mode, although a larger relative deviation

is observed for the maximum displacements, which are nevertheless much smaller (and therefore less important) than those for the parametric resonance of the first mode. It also takes longer for the finite-element response to build up.

When the ‘modal relationships’ (3) are used, any other generalised co-ordinate and velocity of the ‘high-order’ model can be recovered, provided the modal displacement and velocity are known. To illustrate it, the p_{30} generalised co-ordinate is considered. From (3)

$$\begin{aligned} p_{30} &= a_{1,30}^1 U_1 + a_{1,30}^2 U_2 + a_{2,30}^1 \dot{U}_1 + a_{2,30}^2 \dot{U}_2 + a_{3,30}^{11} (U_1)^2 \\ &\quad + a_{3,30}^{22} (U_2)^2 + a_{4,30}^{11} U_1 \dot{U}_1 + a_{4,30}^{22} U_2 \dot{U}_2 + a_{5,30}^{11} (\dot{U}_1)^2 \\ &\quad + a_{5,30}^{22} (\dot{U}_2)^2 + a_{6,30}^{111} (U_1)^3 + a_{6,30}^{222} (U_2)^3 + a_{7,30}^{111} (U_1)^2 \dot{U}_1 \\ &\quad + a_{7,30}^{222} (U_2)^2 \dot{U}_2 + a_{8,30}^{111} U_1 (\dot{U}_1)^2 + a_{8,30}^{222} U_2 (\dot{U}_2)^2 \\ &\quad + a_{9,30}^{111} (\dot{U}_1)^3 + a_{9,30}^{222} (\dot{U}_2)^3 \end{aligned}$$

$$\begin{aligned} \dot{p}_{30} &= b_{1,30}^1 U_1 + b_{1,30}^2 U_2 + b_{2,30}^1 \dot{U}_1 + b_{2,30}^2 \dot{U}_2 + b_{3,30}^{11} (U_1)^2 \\ &\quad + b_{3,30}^{22} (U_2)^2 + b_{4,30}^{11} U_1 \dot{U}_1 + b_{4,30}^{22} U_2 \dot{U}_2 + b_{5,30}^{11} (\dot{U}_1)^2 \\ &\quad + b_{5,30}^{22} (\dot{U}_2)^2 + b_{6,30}^{111} (U_1)^3 + b_{6,30}^{222} (U_2)^3 + b_{7,30}^{111} (U_1)^2 \dot{U}_1 \\ &\quad + b_{7,30}^{222} (U_2)^2 \dot{U}_2 + b_{8,30}^{111} U_1 (\dot{U}_1)^2 + b_{8,30}^{222} U_2 (\dot{U}_2)^2 \\ &\quad + b_{9,30}^{111} (\dot{U}_1)^3 + b_{9,30}^{222} (\dot{U}_2)^3 \end{aligned}$$

with the following non-null coefficients, from *MODONL* [26], for the first mode

$$\begin{aligned} a_{1,30}^1 &= 0.68825E + 00 & a_{2,30}^1 &= -0.88725E - 04 \\ a_{6,30}^{111} &= -0.14670E - 01 & a_{7,30}^{111} &= 0.15287E - 04 \\ a_{8,30}^{111} &= -0.57711E - 03 \\ b_{1,30}^1 &= 0.13842E - 02 & b_{2,30}^1 &= 0.68825E + 00 \\ b_{6,30}^{111} &= -0.19144E - 03 & b_{7,30}^{111} &= -0.26004E - 01 \\ b_{8,30}^{111} &= 0.83664E - 04 & b_{9,30}^{111} &= -0.57710E - 03 \end{aligned}$$

and for the second mode

$$\begin{aligned} a_{1,30}^2 &= 0.23904E + 01 & a_{2,30}^2 &= -0.78791E - 04 \\ a_{6,30}^{222} &= 0.18393E + 00 & a_{7,30}^{222} &= -0.37105E - 03 \\ a_{8,30}^{222} &= 0.70872E - 02 \\ b_{1,30}^2 &= 0.48281E - 01 & b_{2,30}^2 &= 0.23904E + 01 \\ b_{6,30}^{222} &= -0.51047E + 00 & b_{7,30}^{222} &= -0.81337E + 01 \\ b_{8,30}^{222} &= 0.22603E - 02 & b_{9,30}^{222} &= 0.70872E - 02 \end{aligned}$$

For parametric resonance with the first mode, it is seen that the linear terms prevail in the p_{30} and \dot{p}_{30} responses. The non-linear terms have just a moderate influence on them. For parametric resonance with the second mode, besides the linear term, non-linearities – $a_{6,30}^{222} (U_2)^3 + a_{8,30}^{222} U_2 (\dot{U}_2)^2$ – have a clear influence on the p_{30} response. Further, for \dot{p}_{30} , besides the linear term, the non-linearities – $b_{7,30}^{222} (U_2)^2 \dot{U}_2 +$

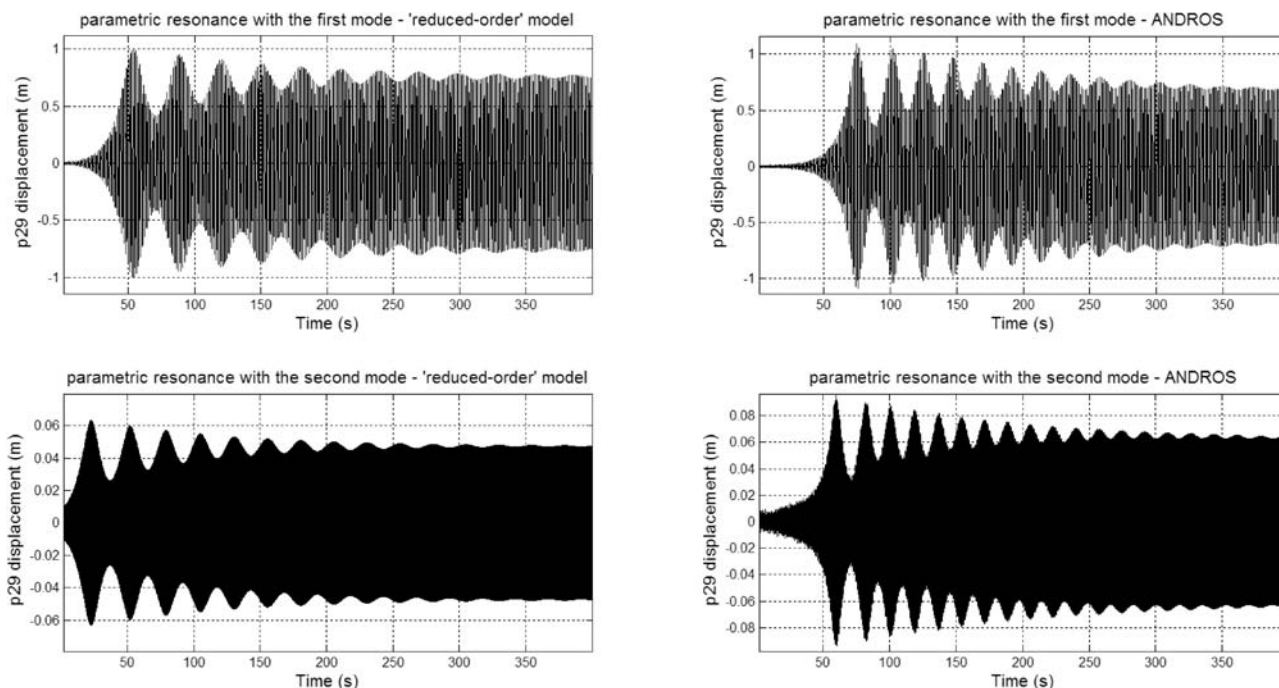


Fig. 8 p_{29} in the ‘reduced-order’ model and *ANDROS*, for parametric resonance with respect to the first or the second mode, $c = 0.01$ Ns/m, $\gamma_0 = 3.0$ m/s²

$b_{8,30}^{222} U_2 (\dot{U}_2)^2 + b_{9,30}^{222} (\dot{U}_2)^3$ – become strongly relevant. It should be recalled that $O(\dot{U}_u) = \omega_{0u} O(U_u)$, which leads to non-linearly-amplified velocity-dependent terms particularly in the second mode, because $\omega_{02} = 24.75$ rad/s is large.

Deviations in the steady-state amplitudes for p_{30} and \dot{p}_{30} , which are evaluated for the ‘reduced-order’ and finite-element models using *ANDROS* [11] were found to be of the same order of those found for p_{29} , in spite of expected propagation errors: for the parametric resonance with the first mode, the ‘reduced-order’ model amplitude is 0.5082 rad and the *ANDROS* amplitude is 0.4677 rad (deviation of 9 per cent); for the parametric resonance with the second mode, the ‘reduced-order’ model amplitude is 0.1515 rad and the *ANDROS* amplitude is 0.1144 rad (deviation of 24 per cent).

Finally, to assess the role played by the velocity contents within the non-linear modes, when it comes to obtain ‘reduced-order’ models, a comparison is shown in Fig. 9 between results with and without it.

Extremely large deviations – more than 92 per cent – in the periodic-attractor displacement amplitudes for parametric resonance with the first mode can be observed in Fig. 9, thus justifying the use of the improved procedure for ‘reduced-order’ modelling. Velocity-dependent terms in the non-linear modes may act either to decrease (for the parametric resonance with respect to the first mode) or increase (for the parametric resonance with respect to the second mode) the response amplitudes. Deviations should,

of course, be much smaller if the structure were not so slender, so lightly damped and also subjected to parametric resonance. Still, the improved procedure to obtain ‘reduced-order’ models is not much more laborious and renders more reliable results than the previously proposed one [9, 10], so that it should be used even when the scenario is not as critical as the one addressed here.

When the forcing frequency is varied in the vicinity of the principal parametric-resonance region (approximately twice the natural frequency of either the first or the second mode) keeping the excitation amplitude constant, a typical Hopf bifurcation pattern is recognizable, as shown in Fig. 10. It is observed that the post-critical behaviour, due to the cubic nonlinearities, is of the hardening type for the parametric resonance with the first mode – as if the overall influence would agree with the term $c_6^{111} (U_1)^3$ – and softening type for the parametric resonance with the second mode – as if the overall influence would agree with the term $c_6^{222} (U_2)^3$, which is a similar scenario to the well-known case of the parametric resonance of the Duffing equation [31].

The expected trace of unstable limit cycles between the stable limit cycles and the trivial (equilibrium) solution for some frequency range could not be captured in the numerical analysis, probably because it is too steep. Except for the region near to the end of the stable post-critical solution, the problem was found to be insensitive to initial conditions.

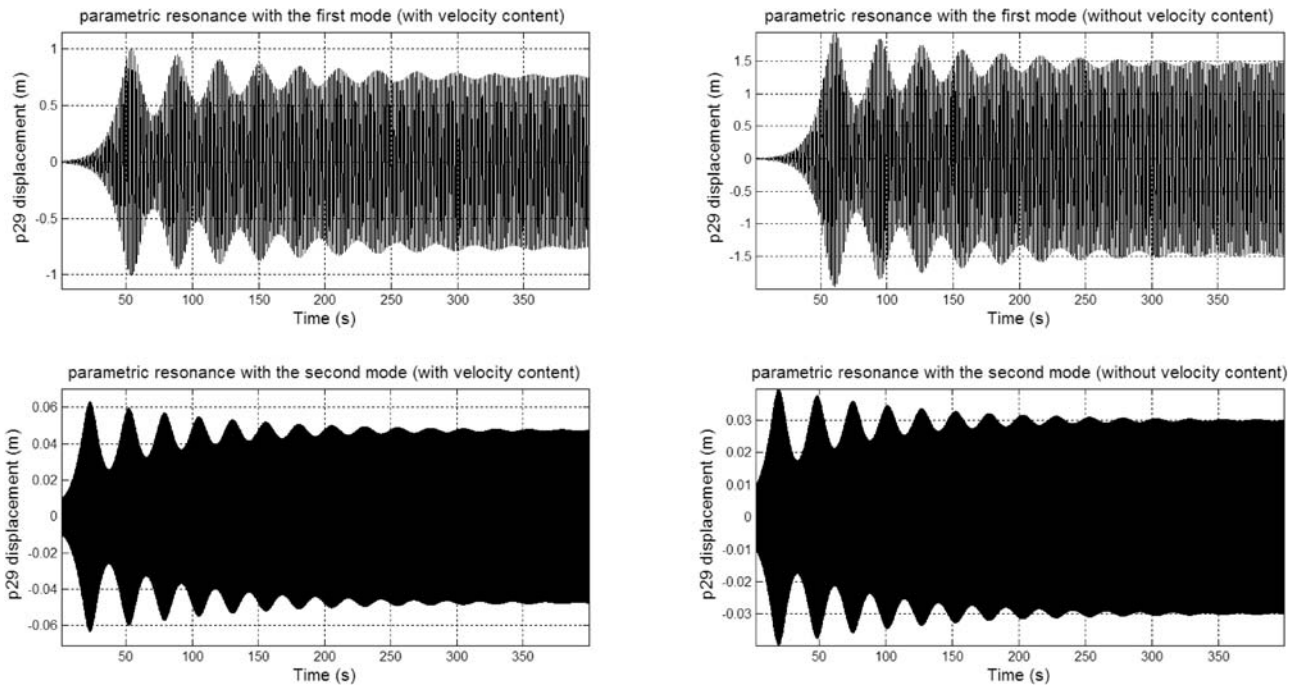


Fig. 9 p_{29} in the ‘reduced-order’ model with or without velocity contents in the non-linear mode, for parametric resonance with respect to the first or the second mode, $c = 0.01 \text{ Ns/m}$, $\gamma_0 = 3.0 \text{ m/s}^2$

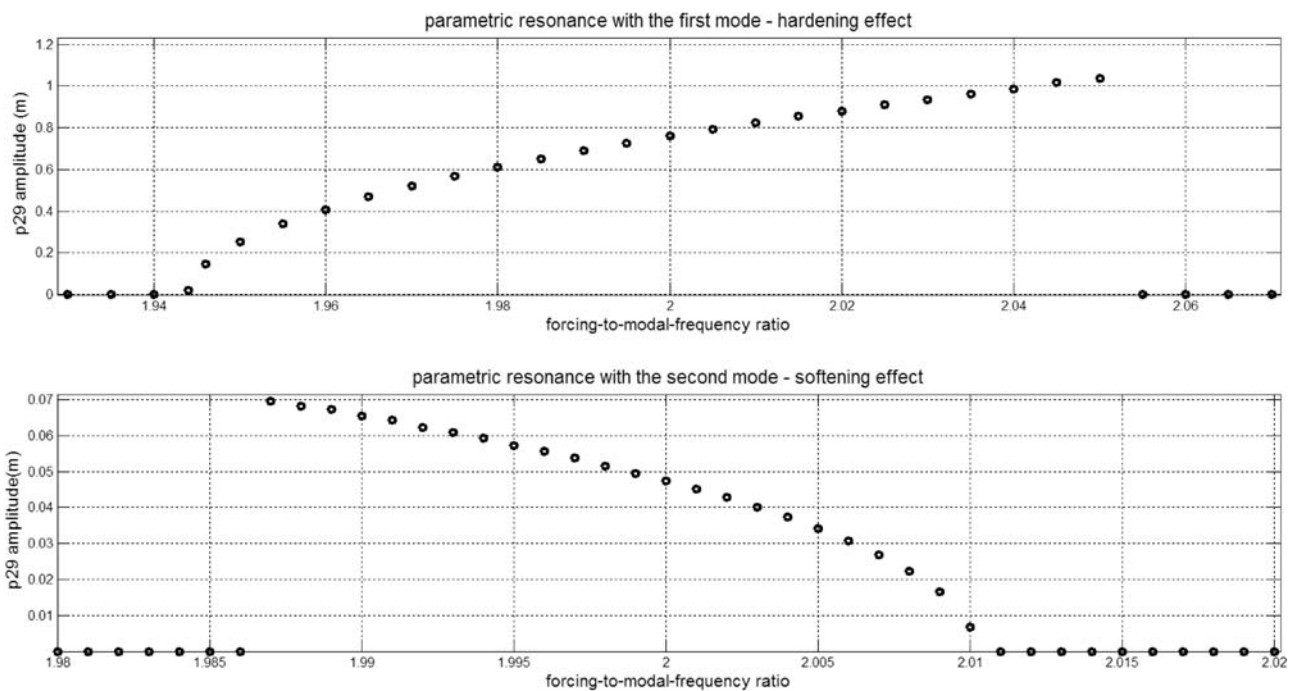


Fig. 10 p_{29} steady-state amplitudes, for the ‘reduced-order’ model, considering parametric resonance with either the first or the second mode, $c = 0.01 \text{ Ns/m}$, $\gamma_0 = 3.0 \text{ m/s}^2$

It is also to be mentioned that varying the forcing frequency ratio around 2:1, and the forcing amplitude in the range 3–9 m/s^2 , for which the post-critical beam displacements could still bear physical meaning, did not show other relevant bifurcation events.

A final word refers to the adequacy of the two-degree-of-freedom ‘reduced-order’ model and to convergence. According to the fast-Fourier transform of the steady-state response under perfectly tuned parametric resonance with the first mode, the

spectral peak ratio is 100.0:6.4 (first-to-second modes), for $c = 0.01 \text{ Ns/m, m/s}^2$. If the third non-linear normal mode is included in the 'reduced-order' model, the spectral peak ratio becomes 100.0:6.2:0.9 (first-to-second-to-third modes), thus indicating a negligible influence of the added mode.

4 CONCLUDING REMARKS

This article addresses an improved procedure for 'reduced-order' modelling in non-linear dynamics. Comparison between non-linear dynamic responses of 'high-order' and 'reduced-order' models under different load conditions is made in two case studies. For both external and parametric resonances, it can be said that a remarkable agreement between them was achieved, provided the velocity contents within the non-linear modes are retained. In the second case study, it is seen that damping is essential to help the system settling down in a post-critical periodic attractor, otherwise wave propagation and reflection, with constructive and destructive composition, will have an enduring effect.

ACKNOWLEDGEMENTS

The authors are grateful to Renato Teixeira Burin for his help with the numerical analysis.

FUNDING

The author Carlos E.N. Mazzilli acknowledges the support of the Brazilian Science Research Council, CNPq, under the grant 301942/2009-9.

© Authors 2011

REFERENCES

- 1 Foias, C., Jolly, M. S., Kevrekidis, I. G., Sell, G. R. R., and Titi, E. S. On the computation of inertial manifolds. *Phys. Lett.*, 1988, **A131**, 433–437.
- 2 Marion, M. and Temam, R. Nonlinear Galerkin methods. *SIAM J. Num. Anal.*, 1989, **26**, 1139–1157.
- 3 Brown, H. S., Jolly, M. S., Kevrekidis, I. G., and Titi, E. S. Use of approximate inertial manifolds in bifurcation calculations. In *Continuation and bifurcations: numerical techniques and applications* (Eds D. Roose, B. De Dier, A. Spence), 1990, pp. 9–23 (Kluwer Academic Publishers, Dordrecht).
- 4 Garcia-Archilla, B., Novo, J., and Titi, E. S. Postprocessing the Galerkin method: a novel approach to approximate inertial manifolds. *SIAM J. Num. Anal.*, 1998, **35**, 941–972.
- 5 Laing, C. R., McRobie, A., Sell, G. R., and Thompson, J. M. T. The post-processed Galerkin method applied to nonlinear shell vibrations. *Dyn. Stab. Syst.*, 1999, **14**, 163–181.
- 6 Touzé, C. and Amabili, M. Nonlinear normal modes for damped geometrically nonlinear systems: application to 'reduced-order' modelling of harmonically forced structures. *J. Sound Vib.*, 2006, **298**, 968–981.
- 7 Amabili, M. and Touzé, C. Reduced-order models for nonlinear vibrations of fluid-filled circular cylindrical shells: comparison of POD and asymptotic nonlinear normal modes methods. *J. Fluids Struct.*, 2007, **23**, 885–903.
- 8 Steindl, A. and Troger, H. Methods for dimension reduction and their application in nonlinear dynamics. *Int. J. Solids Struct.*, 2001, **38**, 2131–2147.
- 9 Mazzilli, C. E. N., Soares, M. E. S., and Baracho Neto, O. G. P. Reduction of finite-element models of planar frames using non-linear normal modes. *Int. J. Solids Struct.*, 2001, **38**, 1993–2008.
- 10 Mazzilli, C. E. N. and Baracho Neto, O. G. P. Finite-element model reduction of an internally resonant portal frame using a non-linear multi-mode. In *Second International Conference on Non-linear normal modes and localization in vibrating systems*, Samos, 19–26 June.
- 11 Brasil, R. M. L. R. F. and Mazzilli, C. E. N. A general formulation of non-linear dynamics applied to accessing the static loading effect upon the dynamic response of planar frames. *Appl. Mech. Rev.*, 1993, **46**, 110–117.
- 12 Rosenberg, R. M. Normal modes of nonlinear dual-mode systems. *J. Appl. Mech.*, 1960, **27**, 263–268.
- 13 Rosenberg, R. M. Normal modes of nonlinear dual-mode systems. *J. Appl. Mech.*, 1962, **29**, 7–14.
- 14 Rosenberg, R. M. On nonlinear vibrations of systems with many degrees of freedom. *Adv. Appl. Mech.*, 1966, **9**, 155–242.
- 15 Vakakis, A. F. *Analysis and identification of linear and nonlinear normal modes in vibrating systems*. PhD Dissertation, California Institute of Technology, Pasadena, California, 1990.
- 16 Vakakis, A. F. Non-similar normal oscillations in a strongly non-linear discrete system. *J. Sound Vib.*, 1992, **159**, 341–361.
- 17 Vakakis, A. F. Non-linear normal modes and their applications in vibration theory: an overview. *Mech. Syst. Signal Proc.*, 1997, **11**, 3–22.
- 18 Shaw, S. W. and Pierre, C. Non-linear normal modes and invariant manifolds. *J. Sound Vib.*, 1991, **150**, 170–173.
- 19 Shaw, S. W. and Pierre, C. Normal modes for non-linear vibratory systems. *J. Sound Vib.*, 1993, **164**, 85–124.
- 20 Shaw, S. W. and Pierre, C. Normal modes of vibration for non-linear continuous systems. *J. Sound Vib.*, 1994, **169**, 319–347.
- 21 Hsu, L. Analysis of critical and post-critical behaviour of nonlinear dynamical systems by the normal form method. Part I: normalization formulae. *J. Sound Vib.*, 1983, **89**, 169–181.
- 22 Hsu, L. Analysis of critical and post-critical behaviour of nonlinear dynamical systems by the normal

form method. Part II: divergence and flutter. *J. Sound Vib.*, 1983, **89**, 183–194.

23 **Jezequel, L.** and **Lamarque, C. H.** Analysis of non-linear structural vibrations by normal form theory. *J. Sound Vib.*, 1991, **149**, 429–459.

24 **Nayfeh, A. H.** On direct methods for constructing nonlinear normal modes of continuous systems. *J. Vib. Control*, 1995, **1**, 389–430.

25 **Mazzilli, C. E. N.** and **Baracho Neto, O. G. P.** Evaluation of non-linear normal modes for finite-element models. *Comp. Struct.*, 2002, **80**, 957–965.

26 **Soares, M. E. S.** and **Mazzilli, C. E. N.** Nonlinear normal modes of planar frames discretised by the finite-element method. *Comp. Struct.*, 2000, **77**, 485–493.

27 **Kerschen, G., Peeters, M., Golinval, J. C., and Vakakis, A. F.** Nonlinear normal modes, Part I: A useful framework for the structural dynamicist. *Mech. Syst. Signal Proc.*, 2009, **23**, 170–194.

28 **Jiang, D., Pierre, C., and Shaw, S. W.** Nonlinear normal modes for vibratory systems under harmonic excitation. *J. Sound Vib.*, 2005, **288**, 791–812.

29 **Baracho Neto, O. G. P.** and **Mazzilli, C. E. N.** Evaluation of multi-modes for finite-element models: systems tuned into 1:2 internal resonance. *Int. J. Solids. Struct.*, 2005, **42**, 5795–5820.

30 **Bolotin, V. V.** *The dynamic stability of elastic systems*, 1964 (Holden Day, San Francisco).

31 **Nayfeh, A. H.** and **Mook, D. T.** *Nonlinear oscillations*, 1979 (John Wiley, New York).

APPENDIX

Notations

$a_{1r}^u, a_{4r}^{uv}, a_{7r}^{uvw}, b_{1r}^u, b_{4r}^{uv}, b_{7r}^{uvw}, c_1^u, c_4^{uv}, c_7^{uvw}, D_{rs}$	$a_{2r}^u, a_{5r}^{uv}, a_{8r}^{uvw}, b_{2r}^u, b_{5r}^{uv}, b_{8r}^{uvw}, c_2^u, c_5^{uv}, c_8^{uvw}$	$a_{3r}^{uv}, a_{6r}^{uvw}, a_{9r}^{uvw}, b_{3r}^{uv}, b_{6r}^{uvw}, b_{9r}^{uvw}, c_3^{uv}, c_6^{uvw}, c_9^{uvw}$	coefficients defining invariant manifold for generalised coordinate p_r and modes u, v, w
			coefficients defining invariant manifold for generalised velocity \dot{p}_r and modes u, v, w
			coefficients defining non-linear equation of motion for mode u
			equivalent damping-matrix element in line r and column s
D_{rs}^0			linear equivalent damping-matrix element in line r and column s
$D_{rsk}^1, D_{rsk\ell}^2$			non-linear equivalent damping-matrix coefficients in line r and column s

E	Young’s modulus
\mathbf{F}_p	generalised-load vector of the ‘high-order’ model
\mathbf{F}_u	generalised-load vector of the ‘reduced-order’ model
h	cross-section height
K_{rs}	stiffness-matrix element in line r and column s
K_{rs}^0	linear stiffness-matrix element in line r and column s
$K_{rsk}^1, K_{rsk\ell}^2$	non-linear stiffness-matrix coefficients in line r and column s
L	beam length
M_{rs}	mass-matrix element in line r and column s
M_{rs}^0	linear mass-matrix element in line r and column s
$M_{rsk}^1, M_{rsk\ell}^2$	non-linear mass-matrix coefficients in line r and column s
M_u	u modal mass
$O(U_u)$ or $O(\dot{U}_u)$	order of the generalised u modal displacement or velocity, respectively
\mathbf{p}	generalised-displacement vector
p_s	generalised displacement of degree of freedom s
\dot{p}_s	generalised velocity of degree of freedom s
\ddot{p}_s	generalised acceleration of degree of freedom s
P_u	u modal acceleration
p_{0s}	generalised displacement of degree of freedom s , for the equilibrium configuration
R_r	generalised force of degree of freedom r
\mathbf{U}	modal displacement vector
$\dot{\mathbf{U}}$	modal velocity vector
U_u	modal displacement of mode u
\dot{U}_u	modal velocity of mode u
\ddot{U}_u	modal acceleration of mode u
γ_0	modal acceleration amplitude
γ_u^r	contribution of generalised force R_r to u modal acceleration
$\delta \mathbf{p}$	generalised virtual-displacement vector
δp_r	generalised virtual-displacement of degree of freedom r

δU_u	virtual u modal-displacement	ξ_u	critical damping ratio of mode u
δW	virtual work	ρ	specific mass
$\delta \mathbf{p}$	generalised virtual-displacement vector	ω_{0u}	linear natural frequency of mode u